Published in final edited form as:
J Vasc Interv Radiol. 2010 April ; 21(4): 555–561. doi:10.1016/j.jvir.2010.01.002.

Preclinical Assessment of a 980-nm Diode Laser Ablation System in a Large Animal Tumor Model

Kamran Ahrar, MD, **Ashok Gowda, PhD**, **Sanaz Javadi, MD**, **Agatha Borne, PhD, DVM**, **Matthew Fox, BS**, **Roger McNichols, PhD**, **Judy U. Ahrar, MD**, **Clifton Stephens, PhD, DVM**, and **R. Jason Stafford, PhD**
From the BioTex, Inc. (A.G., M.F., R.M.), Houston, Texas; the Departments of Radiology, Section of Interventional Radiology (S.J., J.U.A., K.A.); the Department of Veterinary Medicine and Surgery (A.B., C.S.); the Department of Imaging Physics (R.J.S), The University of Texas M.D. Anderson Cancer Center, Houston, Texas

Abstract

Purpose—To characterize the performance of a 980-nm diode laser ablation system in an in vivo tumor model.

Materials and Methods—This study was approved by the Institutional Animal Care and Use Committee. The ablation system consisted of a 15-W, 980-nm diode laser, flexible diffusing tipped fiber optic, and 17-gauge internally cooled catheter. Ten immunosuppressed dogs were inoculated subcutaneously with canine transmissible venereal tumor fragments in eight dorsal locations. Laser ablations were performed at 79 sites where inoculations were successful (99%) using powers of 10 W, 12.5 W, and 15 W, with exposure times between 60 and 180 seconds. In 20 cases, multiple overlapping ablations were performed. After the dogs were euthanized, the tumors were harvested, sectioned along the applicator track, measured and photographed. Measurements of ablation zone were performed on gross specimen. Histopathology and viability staining was performed using hematoxylin and eosin (H&E) and nicotinamide adenine dinucleotide hydrogen (NADH) staining.

Results—Gross pathology confirmed well-circumscribed ablation zone with sharp boundaries between thermally ablated tumor in the center surrounded by viable tumor tissue. When a single applicator was used, the greatest ablation diameters ranged from 12 mm at the lowest dose (10 W, 60 sec) to 26 mm at the highest dose (15 W, 180 sec). Multiple applicators created ablation zones of up to 42 mm in greatest diameter (with the lasers operating at 15 W for 120 sec).

Conclusions—The new 980-nm diode laser and internally cooled applicator effectively creates large ellipsoid thermal ablations in less than 3 minutes.

INTRODUCTION

Laser ablation is a minimally invasive therapy that has been used to successfully ablate tumors in several tissues, including the liver (1), brain (2), thyroid (3), bone (4), and others (5). Lasers operate by depositing light energy, which is absorbed by tissue components, thus generating volumetric heat (6). Small-diameter silica fiber optics are able to carry large amounts of energy, making them well-suited for minimally invasive ablation procedures. Such fibers are usually

compatible with magnetic resonance imaging (MRI) systems, allowing their use during thermal image-guided applications (7,8). Two different laser systems have been used for tumor ablation. The Nd:YAG (neodymium-doped yttrium aluminum garnet) laser is a solid-state laser which operates by stimulating light emission from an Nd:YAG crystal, which serves as its active laser medium. The light amplification (or gain) results from the stimulated emission of electronic or molecular transitions to a lower energy state from a higher energy state. This process often requires higher currents and therefore larger power supplies (220 volts) as well as active water cooling for the laser, resulting in fewer areas that the laser can be operated. Diode-based lasers on the other hand use a semiconductor as the active medium. This reduces dramatically the power and cooling requirements allowing the lasers to be operated with 110 voltage supply with air cooling only. In addition, the Nd:YAG laser operates at 1,064-nm and at this wavelength, water (which is a major component of tissue) exhibits an absorption coefficient of 0.144 cm^{-1}. By contrast, the water absorption coefficient at 980 nm is 0.482 cm^{-1}. Since the rate of optical thermal generation in tissue is proportional to the absorption coefficient and the fluence rate, the 980-nm diode laser is capable of producing rapid and localized heating of tissue and thereby creating ablation zones with sharp boundaries using relatively low powers. The most commonly used laser in previous investigations was the Nd:YAG laser operating at 1064 nm (9). Most ND:YAG laser ablation systems described in the previous literature required significant exposure times up to 37 minutes (range 15–37 minutes, mean 23 minutes) and high power levels to create effective thermal ablation zones (10). Others have used multiple fibers (up to four) with exposure times of 6 to 12 minutes (11). Laser fibers have been used in conjunction with internal cooling catheters, allowing use of even higher laser powers and exposure durations (12). However, placement of cooling catheters required larger-diameter applicators (2–3 mm). Thus, there is a need for laser ablation systems that are smaller, work more rapidly, and require less energy for effective tumor ablation. Newer infrared diode-based systems operating in the range of 805 nm – 980 nm utilize smaller applicators, and create larger ablation zones in shorter periods of time (13,14). Therefore the purpose of the current study was to characterize the performance of a new 980-nm diode laser ablation system in a large animal tumor model.

Materials and Methods

Laser Ablation System

The laser ablation system used in this study consists of a commercially available 980-nm diode laser ($PhoTex_{15}$; Visualase, Inc., Houston, TX) and disposable applicator set (Visualase Cooled Laser Applicator System [VCLAS]; Visualase). An irrigation pump (K-Pump; Kolster Methods Inc., Corona, CA) was used to supply room-temperature sterile saline to the laser applicator. The $PhoTex_{15}$ operates in continuous-wave mode with a maximum output power of 15 W (Fig 1).

The VCLAS disposable applicator set consists of a 400-μm core fiber optic equipped with an integrated cylindrical 10-mm-long diffusing tip element (Fig 2). The outer diameter of the diffusing fiber is 0.76 mm (< 21 gauge). The cylindrical diffusing tip scatters light in an approximately cylindrical pattern over its length, leading to an elliptical heating volume. A cooling catheter is used to circulate room-temperature saline over the fiber and remove heat from both the fiber and the center of the ablation zone during treatment. The cooling catheter is approximately 1.6 mm in diameter (17 gauge), with a usable length of 27.5 cm. The applicator can be placed in coaxial fashion using a 14-gauge guide needle system. A pump tubing set and fluid collection reservoir are used to deliver sterile fluid to the cooling catheter and store returned fluids. The pump is operated to maintain a flow rate of between 15 and 20 ml/min of room-temperature (22–25°C) saline.

Animal Tumor Model

To evaluate the performance of the laser and applicator system, we employed a subcutaneous canine transmissible venereal tumor (c-TVT) model to mimic a relevant tumor tissue environment (15). This study was approved by the Institutional Animal Care and Use Committee, and the animals were handled in compliance with recommendations of the "Guide for the Care and Use of Laboratory Animals" (16). Ten 29–39-kg dogs were used in the study. The animals were treated with 10 mg/kg oral cyclosporine (Sandimmune; Novartis Pharmaceutical Corp., East Hanover, NJ) twice per day until tumor inoculation (9–16 days, mean=12 days). The dogs were placed under general anesthesia, and the dorsal vertebral and paravertebral areas were sterilized in preparation for tumor inoculation. Each animal was inoculated in eight locations with 0.5 mL of freshly prepared c-TVT slurry previously obtained from donor animals. Four inoculates were each placed subcutaneously approximately 5 cm from the dorsal midline and 10 cm apart in both the right and left paravertebral locations, for a total of eight inoculations per animal. After tumor inoculation, the oral cyclosporine dose was decreased to 10 mg/kg once per day for the remainder of the study. Tumor growth was monitored by palpation, and laser therapy was scheduled when the largest tumors were at least 5 cm or the smallest was over 2 cm (approximately 6 weeks).

Anesthesia during Ablation

When the tumors reached the appropriate size for treatment, the animals were pre-anesthetized with acepromazine (0.1 mg/kg, IM) and atropine (0.04 mg/kg, IM); full anesthesia was induced with thiopental (Pentothal; 16 mg/kg, IV) and maintained with isoflurane administered at a concentration of 1–3% in oxygen.

Applicator Placement and Laser Delivery

To facilitate introduction of the applicator and proper sectioning of the ablation zone, we used a 14-gauge (2.1 mm) intravenous catheter (Abbocath-T; Hospira, Inc., Austin, TX) as a guide. Each fiber was placed in a coaxial fashion using the 14-gauge guide catheter. We planned a total of 80 laser ablations. The primary goal of this study was to characterize the performance of the system with a single applicator after a single ablation. Therefore, 60 ablations were planned using three different power settings (10 W, 12.5 W, and 15 W) with four different ablation times (60, 90, 120, and 150 sec). In 9 tumors a single applicator was introduced and was pulled back after each ablation at increments of 1 cm, 1.5 cm, or 2 cm. The laser was operated at 15 W for 60, 90, or 120 seconds. In 11 tumors, two applicators were introduced in parallel separated by 1.5 cm (10 tumors) or 2.5 cm (1 tumor). The laser was operated at 15 W for 60, 90, or 120 seconds. In 10 cases, ultrasound guidance was used to guide insertion of the laser applicator to the center of tumor. Images were acquired using a HDI 5000 ultrasonography system (Philips-ATL, Bothell, WA) with a high-frequency linear array transducer (model L12-5). In the remainder of the cases, the applicators were placed within the center of the tumor under palpation guidance. After placing the fibers, the pump was engaged and sterile saline was allowed to flow through the applicator.

Animal Sacrifice and Tissue Removal

Animals were maintained under anesthesia for at least 90 minutes after completion of the last thermal ablation to allow maturation of ablation zones and development of a visible hyperemic ring indicating the extent of coagulative necrosis. Animals were then euthanized by anesthetic overdose (barbiturate and/or isoflurane) and exsanguination. Each tumor was harvested in whole and a pathology blade was used to section the tumor along the length of the applicator track at the center of the ablation zone.

Ablation Dimensions and Volume Determination

The two greatest dimensions of the ablation zone, along the length of the applicator and perpendicular to the applicator, were measured using digital calipers (Mitutoyo Corporation, Kanagawa, Japan). This measurement instrument provides values to 1/100 of a mm. All measurements were rounded up to a tenth of a millimeter. Mean values were calculated with the numbers rounded up to a tenth of a millimeter. Measurements were taken to the outer border of the hyperemic ring as determined by visual inspection. Previous studies have shown that this border separates normal from heat-induced coagulated tissue (17–20). These measurements (x, y and z, assuming a cylindrical ablation where x and y are equal) were used to calculate the volume of an ellipsoid using following formula: $[(4\Pi/3)(x/2)(y/2)(z/2)]$ (21).

Histology

Ablation zones were measured, photographed grossly, and tagged prior to storage in 10% buffered formalin for later histological analysis. Sectioned tissue samples from eight ablation zones were snap frozen in liquid nitrogen in preparation for viability staining with nicotinamide adenine dinucleotide (NADH). Contiguous ablations for multiple applicators or multiple dose ablation zones were assessed both grossly and by use of NADH staining. On gross inspection a single uniform hyperemic ring encompassing the entire ablation zone was observed for a contiguous ablation, whereas non-contiguous ablations would be identified by a dip in the ring between ablation zones or two opposing rings between ablation zones. Histological analysis using H & E staining under light microscopy was performed to examine and confirm areas of thermal damage. NADH (viability) staining was used to confirm cell death in areas between applicators in cases of multiple applicator ablations and between the ablation zones for individual lesions, as would be caused by fiber pullback (22).

Statistical Analysis

Numerical data was tabulated in a spreadsheet database (Excel, Microsoft Office version 2003). Mean, median, and standard deviation values were calculated.

RESULTS

Lesion Dosimetry

A total of 79 ablations were made in this study, one tumor did not undergo ablation because of its small size. All ablations were created without complication or failures of the applicator system. In five cases, the ablation zones extended to the boundary of the tumor, precluding accurate measurement of the ablation zone. Measurements for these 5 tumors were not included in the analysis of mean ablation length, width, or volume. In 2 tumors, the ablation was carried out beyond the maximum intended duration of 180 seconds. Measurements for these two tumors were not included in the analysis. In 57 ablations, a single applicator was placed and a single laser irradiation was performed (Fig 3a). The laser power varied from 10 to 15 W, and the duration of the ablation varied from 60 to 180 seconds. The size of the ablation zone increased as a function of power and time (table). Applying 15 W of power for a maximum of 3 minutes resulted in a mean ablation zone of 24.6 × 25.8 mm (SD = 1.6 mm).

Repositioning of the fiber at 1-cm increments along the length of the applicator resulted in contiguous ablation even after a short exposure (60 sec). When the fiber was pulled back 1.5 cm, complete and contiguous ablation was achieved after 2 minutes of laser exposure. When the fiber was pulled back 2 cm, an exposure of 2 minutes resulted in partially contiguous ablation zones (Fig 3b).

Similarly, placing two applicators side-by-side, separating the fibers by 1.5 cm, resulted in complete and contiguous ablation in the area between the applicators after 2 minutes of

exposure (Fig 3c). The average width of the ablation zone was measured as 35 mm (median 36 mm, range: 32–36 mm) and the average length was 36.5 mm (median 37.5 mm, range: 29.4–41.7 mm) after 2 minutes of 15 W ablation with 2 applicators. In one case, where applicators were separated by 2.5 cm, an exposure of 2 minutes at 15 W did not achieve complete coagulation in the area between the applicators.

Gross Pathology and Histopathology

On gross examination of tumors (n = 79), the laser ablation zones were spherical or ellipsoidal, with sharp boundaries between ablated and non-ablated tissue (Fig 3). The center of the ablation zone was identified by a highly visible track left by the applicator. A red hyperemic ring was visible around the lesions, denoting the outer boundary of thermal necrosis.

The morphology of a typical c-TVT is shown in Fig 4, and the same tumor rendered necrotic by ablation is illustrated in Fig 5. NADH viability staining (Fig 6) was done in eight tumors to investigate and verify thermal necrosis in the ablation zone and in the potential watershed areas between multiple ablation zones created with a single fiber or in areas between two applicators. On light microscopy, viable tumor cells stained with NADH in an easily identifiable purple hue, whereas completely ablated areas were unstained. Two serial ablations created using a single applicator in which the fiber optic was pulled back within the cooling catheter by 1.0 cm between 15-W, 60-second exposures demonstrated complete ablation along the applicator track when investigated by NADH staining. Similar results were achieved in the areas between multiple applicators separated by 1.5 cm when the laser was operated at 15 W for 120 seconds.

DISCUSSION

We demonstrated that a single 980-nm diode laser and internally cooled laser applicator system was able to generate clinically meaningful ablation zones (up to 25 mm in largest diameter) in a short time period (180 sec) in a tumor model without charring or vaporization. Larger ablations are possible with multiple applicators and/or multiple overlapping ablations.

Laser ablation of tissue occurs by absorption of light energy causing volumetric heating. Light absorption in tissue is dependent on the wavelength of light and the optical properties of the tissue (23). The method and applicator used to apply laser energy can have a dramatic effect on heating and subsequent tissue changes.

Internally cooled applicator systems like the one used is this study are useful in preventing charring or carbonization and allowing use of higher laser powers and larger amounts of energy to be delivered to the tissue over a given time period. In this approach, cooling tissue adjacent to the applicator also allows the highest temperatures to be shifted deeper in the tissue, thereby creating larger ablation zones.

When compared to systems using bare fiber optics, this system, which incorporated a diffusing tip element, caused less charring of the tissue immediately surrounding the laser source, resulting in a larger area of ablation (14).

Another unique feature of this system is its 980-nm wavelength. Water, which is the primary absorber of laser energy in tissues, has a high absorption peak at 980 nm (24). Water is the largest component in tissue and its content may be more consistent than that of other absorbers at this wavelength, such as blood. As such, one should experience more consistent ablation zones among various tissue types using lasers operating at this wavelength than at other wavelengths. The absorption coefficient for water at 980 nm is 3 times higher than that at 1064 nm (0.482 cm^{-1} vs. 0.144 cm^{-1}), which may contribute to the rapid heating and sharp thermal

gradients observed during tissue ablation using the system tested here. More rapid heating of tissue using laser energy may help overcome the convective cooling associated with heat sinks typically experienced during ablation regimens near vascular structures. For electro-conductive ablation technology, such rapid heating may result in gas formation near the ablation electrode and hence an increase in tissue impedance and lowered ablation efficiency (25).

The applicator system used in this study, which had a diameter of 1.6 mm (approximately 17 gauge), was constructed completely from glass and plastics, rendering it compatible with all imaging technologies, including CT, ultrasound, and even MRI. Its greatest potential is for use in an interventional MRI suite, where real-time monitoring of the ablation zone can be performed using MRI-guided thermal mapping.

In general, an ideal ablation system should be capable of achieving large, well-circumscribed, predictable ablation geometry in as little time as possible. We have demonstrated that using a single applicator and a single exposure, we can achieve an ablation zone of 2 cm in diameter in a maximum of 2 minutes. Slightly longer exposure (3 minutes total) can increase the ablation zone to 2.5 cm in longest diameter. We also demonstrated that multiple overlapping ablations can be created along the long axis of the applicator with this rapid laser ablation system. Furthermore, multiple applicators can be placed and operated simultaneously, further reducing the time required for complete ablation of larger tumors. The major concern that might arise regarding use of multiple applicators is whether the tumor tissue between the applicators can be consistently and completely ablated. Tissue viability staining with NADH performed in this study demonstrated that such ablation could be reliably achieved by using spacing of up to 1.5 cm between applicators when the lasers were operated at 15W for 120 seconds.

Vogl et al. used an internally cooled laser applicator in what is the largest study of laser tumor ablation in 899 patients with colorectal liver metastases (26). They used a 1064-nm Nd:YAG laser (Dornier, Medizintechnik, Germering, Germany) in conjunction with a 9 French (3-mm-diameter) cooled applicator system (SOMATEX, Berlin, Germany). High laser powers up to 35 W with exposure times of 28 minutes were employed in that work. In many cases, multiple applicators were used to cover large metastases. It is worth noting that the combined diffusing tip and cooling catheter used by Vogl et al. measured almost double the size of the catheter used in the current study. In addition, many of the ablations created by Vogl et al. required over 20 minutes of laser delivery. Puls, et. al. treated 180 liver metastases from colorectal carcinoma using the same laser and applicator system used by Vogl et al. (27). Similar ablation times (between 20–28 minutes) were used to create therapeutic ablation zones in their study. One of the major limitations noted by the authors was the overall procedure time of between 60 and 120 minutes.

In a preclinical study, Nikfarjam et al. compared the efficacy of diode and Nd:YAG laser systems using bare fibers without a cooling mechanism at low power (2 W) (14). The size of ablation zone, although it was limited (5.9 mm) because of charring, was comparable for the two systems. However, the treatment time was significantly shorter with the diode laser. In our study we have demonstrated that by using an internally cooled applicator and a diffusing tip, larger power sources (up to 15 W) can be used, allowing for creation of ablation zones four times larger (25 mm) than those reported by Nikfarjam et al.

Our study has few limitations. The use of the c-TVT model in this study is both an advantage and a limitation. On one hand, the c-TVT model may be more representative of the optical properties of target tumors and may result in more accurate ablation dosimetry than assessments made in non-tumor bearing organs. On the other hand, the thermal susceptibility of c-TVT may be different from that of common human tumors treated with percutaneous thermal ablation. It is almost certain that the vascularity and perfusion rates for c-TVT are different than those

for human tumors. And finally, the effect of surrounding organs on thermal conduction in this subcutaneous tumor model is not comparable to that of most human tumors. The results of this preclinical study therefore must be validated in cancer patients. Another limitation of this study is the lack of direct comparison of Nd:YAG and diode laser ablation systems. While prior investigations using Nd:YAG lasers and cooled applicators for accomplishing laser ablation required higher powers and longer exposure times (12,27) than those used in the current study, the lack of a direct comparison in the same model and under the same conditions renders the results of improved ablation efficiency at 980-nm unproven. The local tissue optical properties can have a significant impact on ablation zone size for a particular wavelength, and therefore the results of this study can not be generalized to all organs or tumor pathologies.

In summary, we demonstrated reproducible thermal ablation in a large animal tumor model using 980-nm diode laser ablation system. This laser ablation system can create large ellipsoid ablation zone in less than 3 minutes.

Acknowledgments

This work was supported by SBIR grant (2 R44 CA096227-02) from NIH. A.G., M.F., R.M. are shareholders in BioTex, Inc. K.A. and R.J.S. have receicved research support from Biotex.

REFERENCES

1. Vogl TJ, Straub R, Eichler K, Sollner O, Mack MG. Colorectal carcinoma metastases in liver: laser-induced interstitial thermotherapy--local tumor control rate and survival data. Radiology 2004;230:450–458. [PubMed: 14688400]
2. Schwarzmaier HJ, Eickmeyer F, von Tempelhoff W, et al. MR-guided laser-induced interstitial thermotherapy of recurrent glioblastoma multiforme: preliminary results in 16 patients. Eur J Radiol 2006;59:208–215. [PubMed: 16854549]
3. Papini E, Guglielmi R, Bizzarri G, et al. Treatment of benign cold thyroid nodules: a randomized clinical trial of percutaneous laser ablation versus levothyroxine therapy or follow-up. Thyroid 2007;17:229–235. [PubMed: 17381356]
4. Gangi A, Alizadeh H, Wong L, Buy X, Dietemann JL, Roy C. Osteoid osteoma: percutaneous laser ablation and follow-up in 114 patients. Radiology 2007;242:293–301. [PubMed: 17090708]
5. Vogl TJ, Lehnert T, Eichler K, Proschek D, Floter J, Mack MG. Adrenal metastases: CT-guided and MR-thermometry-controlled laser-induced interstitial thermotherapy. Eur Radiol 2007;17:2020–2027. [PubMed: 17180325]
6. Gnyawali SC, Chen Y, Wu F, et al. Temperature measurement on tissue surface during laser irradiation. Med Biol Eng Comput 2008;46:159–168. [PubMed: 17891430]
7. Vogl TJ, Muller PK, Hammerstingl R, et al. Malignant liver tumors treated with MR imaging-guided laser-induced thermotherapy: technique and prospective results. Radiology 1995;196:257–265. [PubMed: 7540310]
8. Vogl TJ, Naguib NN, Eichler K, Lehnert T, Ackermann H, Mack MG. Volumetric evaluation of liver metastases after thermal ablation: long-term results following MR-guided laser-induced thermotherapy. Radiology 2008;249:865–871. [PubMed: 18812558]
9. Norberto L, Polese L, Angriman I, Erroi F, Cecchetto A, D'Amico DF. Laser photoablation of colorectal adenomas: a 12-year experience. Surg Endosc 2005;19:1045–1048. [PubMed: 15942811]
10. Pech M, Wieners G, Freund T, et al. MR-guided interstitial laser thermotherapy of colorectal liver metastases: efficiency, safety and patient survival. Eur J Med Res 2007;12:161–168. [PubMed: 17509960]
11. Pacella CM, Bizzarri G, Magnolfi F, et al. Laser thermal ablation in the treatment of small hepatocellular carcinoma: results in 74 patients. Radiology 2001;221:712–720. [PubMed: 11719667]
12. Vogl TJ, Mack MG, Roggan A, et al. Internally cooled power laser for MR-guided interstitial laser-induced thermotherapy of liver lesions: initial clinical results. Radiology 1998;209:381–385. [PubMed: 9807562]

13. Jiang SC, Zhang XX. Dynamic modeling of photothermal interactions for laser-induced interstitial thermotherapy: parameter sensitivity analysis. Lasers Med Sci 2005;20:122–131. [PubMed: 16328097]

14. Nikfarjam M, Malcontenti-Wilson C, Christophi C. Comparison of 980- and 1064-nm wavelengths for interstitial laser thermotherapy of the liver. Photomed Laser Surg 2005;23:284–288. [PubMed: 15954816]

15. Rivera B, Ahrar K, Kangasniemi MM, Hazle JD, Price RE. Canine transmissible venereal tumor: a large-animal transplantable tumor model. Comp Med 2005;55:335–343. [PubMed: 16158909]

16. Institute of Laboratory Animal Resources, Commission on Life Sciences, National Research Council. Guide for the Care and Use of Laboratory Animals. Washington, D.C.: National Academy Press; 1996.

17. Ahmed M, Lobo SM, Weinstein J, et al. Improved coagulation with saline solution pretreatment during radiofrequency tumor ablation in a canine model. J Vasc Interv Radiol 2002;13:717–724. [PubMed: 12119331]

18. Kruskal JB, Oliver B, Huertas JC, Goldberg SN. Dynamic intrahepatic flow and cellular alterations during radiofrequency ablation of liver tissue in mice. J Vasc Interv Radiol 2001;12:1193–1201. [PubMed: 11585886]

19. McGahan JP, Browning PD, Brock JM, Tesluk H. Hepatic ablation using radiofrequency electrocautery. Invest Radiol 1990;25:267–270. [PubMed: 2185179]

20. Rossi S, Di Stasi M, Buscarini E, et al. Percutaneous RF interstitial thermal ablation in the treatment of hepatic cancer. AJR Am J Roentgenol 1996;167:759–768. [PubMed: 8751696]

21. Dachman AH, MacEneaney PM, Adedipe A, Carlin M, Schumm LP. Tumor size on computed tomography scans: is one measurement enough? Cancer 2001;91:555–560. [PubMed: 11169938]

22. Carson, FL. Histotechnology, a self-instructional text. 2nd ed. Chicago, IL: ASCP Press; 1997. Enzyme histochemistry; p. 264-265.

23. Giering, K.; Minet, O.; Lamprecht, I.; Muller, G. Review of thermal properties of biological tissues. In: Muller, G.; Roggan, A., editors. Laser-induced interstitial thermotherapy. Bellingham, Wash: SPIE Press; 1995. p. 45-65.

24. Roggan, A.; Dorschel, K.; Minet, O.; Wolff, D.; Muller, G. The optical properties of biological tissue in the near infrared wavelength range. In: Muller, G.; Roggan, A., editors. Laser-induced interstitial therapy. Bellingham, Wash: SPIE Press; 1995. p. 10-44.

25. Iizuka MN, Vitkin IA, Kolios MC, Sherar MD. The effects of dynamic optical properties during interstitial laser photocoagulation. Phys Med Biol 2000;45:1335–1357. [PubMed: 10843108]

26. Vogl TJ, Straub R, Eichler K, Woitaschek D, Mack MG. Malignant liver tumors treated with MR imaging-guided laser-induced thermotherapy: experience with complications in 899 patients (2,520 lesions). Radiology 2002;225:367–377. [PubMed: 12409568]

27. Puls R, Langner S, Rosenberg C, et al. Laser ablation of liver metastases from colorectal cancer with MR thermometry: 5-year survival. J Vasc Interv Radiol 2009;20:225–234. [PubMed: 19109037]

Figure 1.
Laser ablation unit consists of a 980-nm diode laser, an irrigation pump, and disposable cooled laser applicator set.

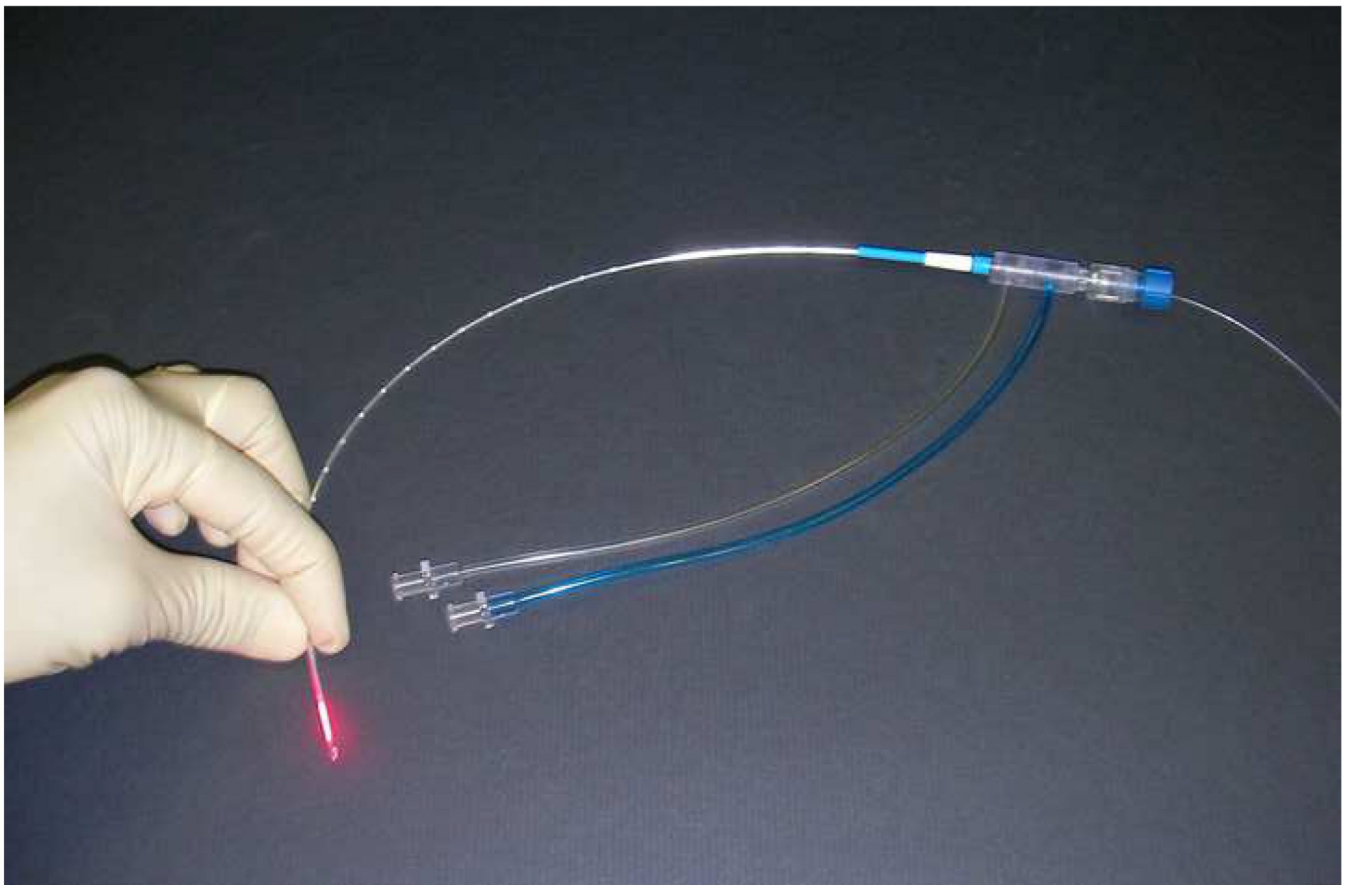

Figure 2.
The Visualase Cooled Laser Applicator System (VCLAS) consists of a 400-μm core fiber optic equipped with an integrated cylindrical 10-mm-long diffusing tip element. The cooling catheter is used to circulate room-temperature saline over the fiber and remove heat from both the fiber and the center of the ablation zone during treatment.

Figure 3a

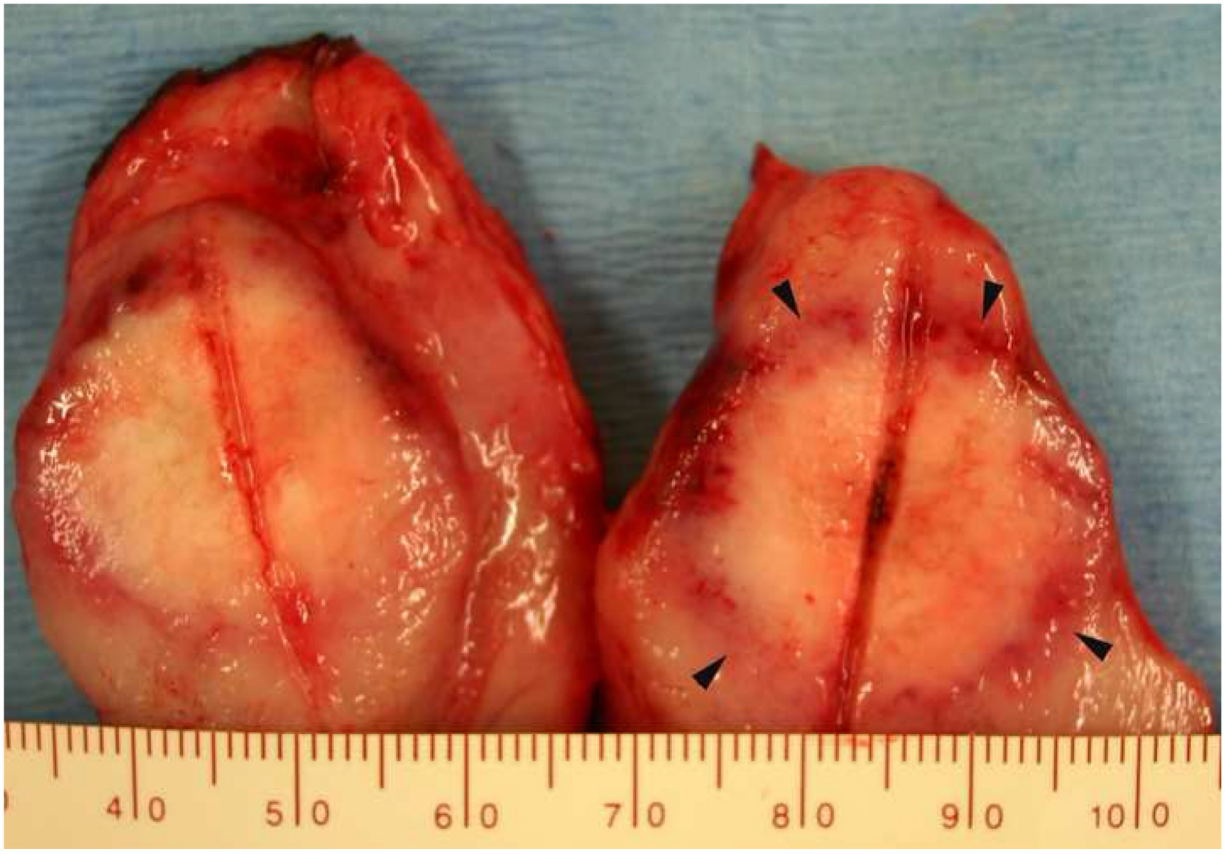

Figure 3b

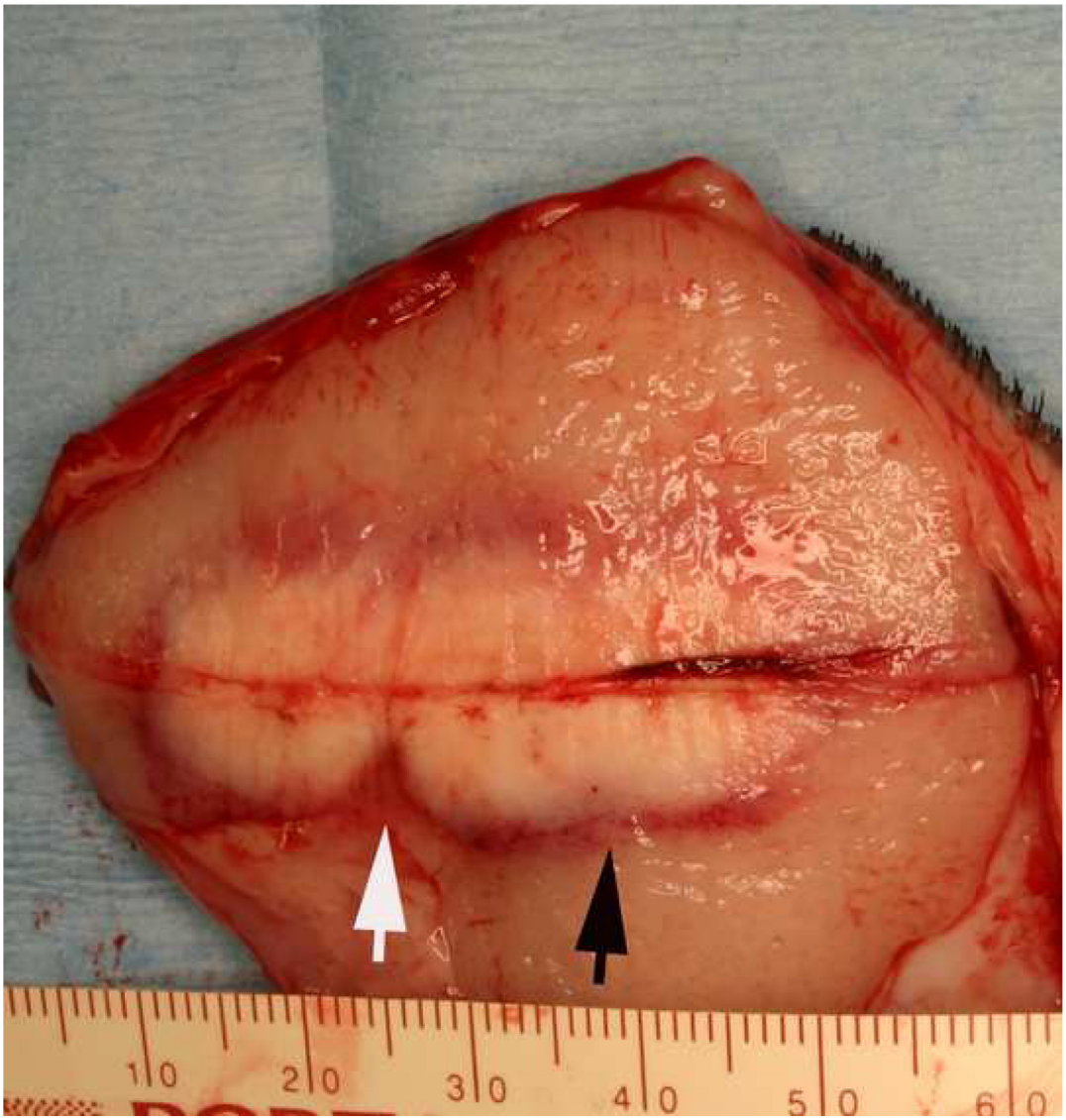

Figure 3c

Figure 3.

Typical ablation created with a single-applicator (a), single-exposure of 15 W for 120 seconds. The lesion shown (arrowheads) measures 20 mm × 23 mm in gross dimensions and contained an estimated thermally coagulated volume of 4987 mm^3. Overlapping ablations were created by pull-back technique (b). Pulling back 1 or 1.5 cm resulted in contiguous ablation (black arrow) while pulling back 2 cm resulted in non-contiguous ablation zone (white arrow). Larger ablations were created with two applicators placed in parallel, separated by 1.5 cm (c). The ablation was performed with both fibers activated at 15 W for 120 seconds at two stations (total ablation time 240 seconds). The ablation zone measured 37 mm × 32 mm. Applicator tracks are seen as two parallel horizontal lines.

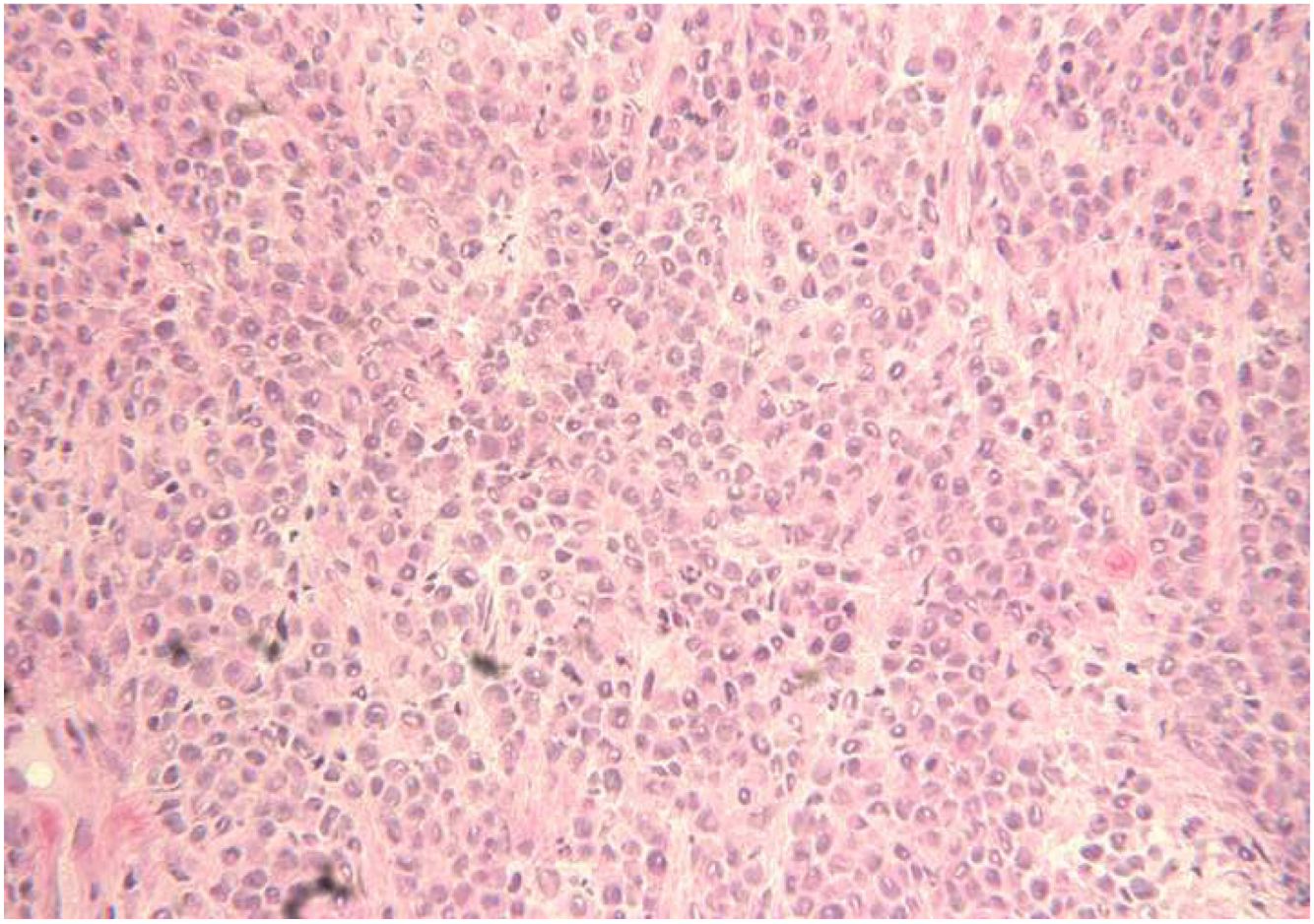

Figure 4.
The viable c-TVT was composed of closely spaced polyhedral-shaped cells with pleomorphic nuclei. Hematoxylin and eosin stain; original magnification, ×250.

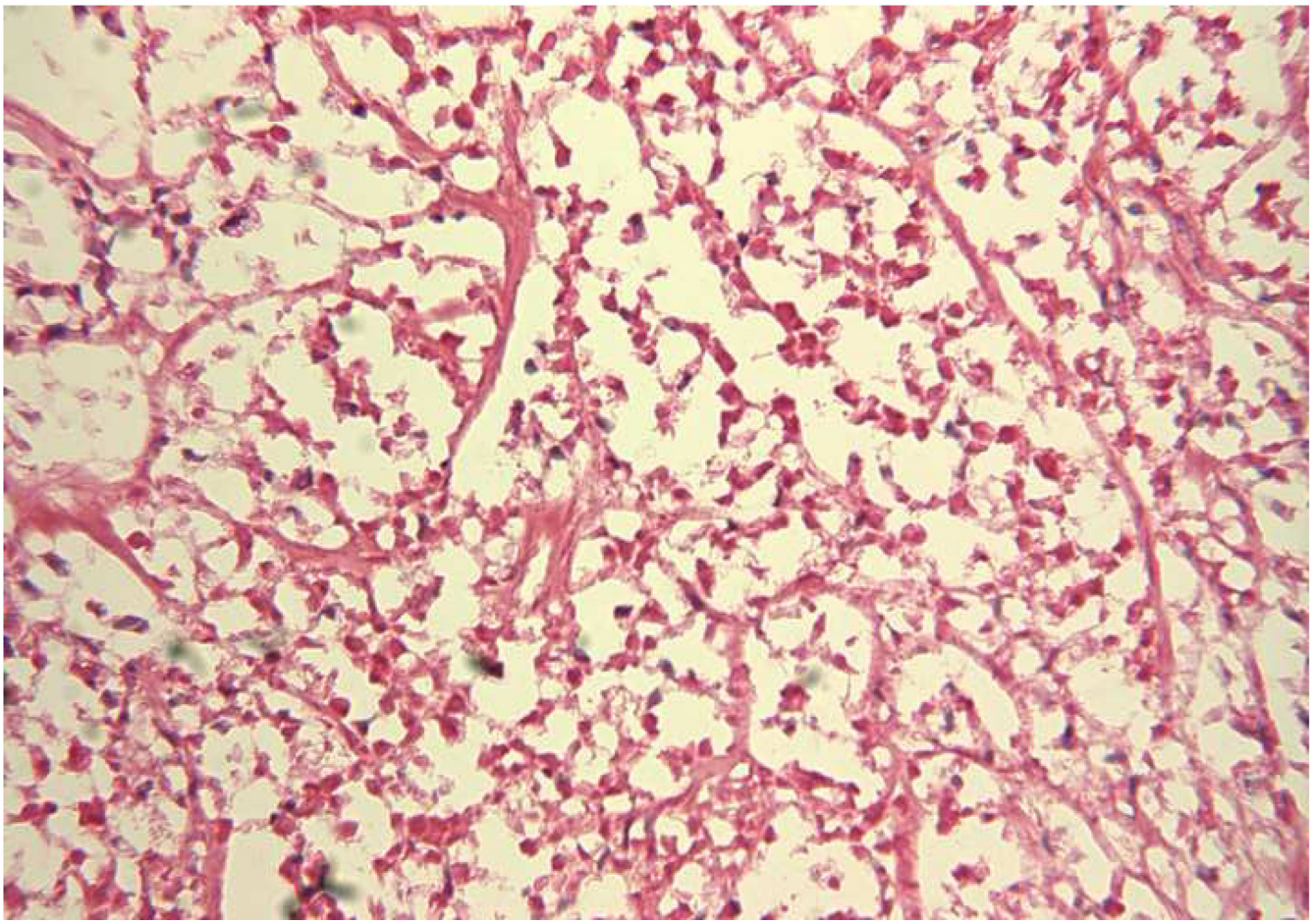

Figure 5.
The necrotic tumor has lost cells and the remaining cells are shrunken and eosinophilic, and many have missing nuclei. Hematoxylin and eosin stain; original magnification, ×250.

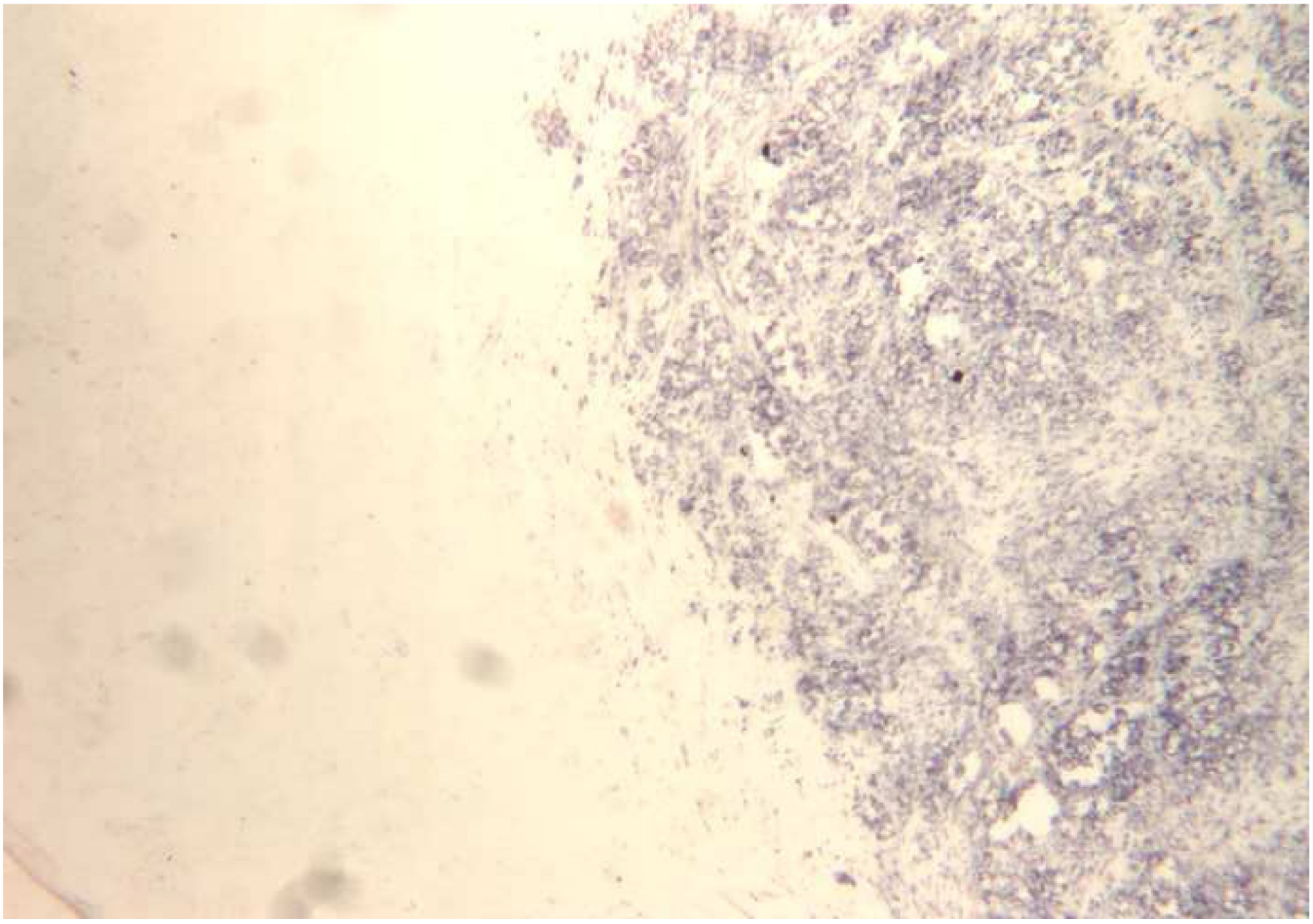

Figure 6.
Fairly abrupt transition between stained, viable cells and unstained, necrotic tumor. NADH stain; original magnification, ×100.

Single Applicator/Single Exposure Ablation Measurements

		Exposure Time (seconds)														
		60			90			120			150			180		
		W*	L†	V‡	W	L	V	W	L	V	W	L	V	W	L	V
Power (W)																
10	Mean	11.6	11.9	848	14.3	14.5	1556	17.1	16.6	2532	17.8	18.5	3113	20.4	22.3	4821
	SD£	0.9	0.2	145	0.3	2.1	275	1.2	0.1	356	1.2	3.8	863	0.1	1.8	350
12.5	Mean	13.3	13.3	1249	16.2	17.0	2382	20.3	21.0	4529	20.5	21.0	4676	21.2	22.2	5197
	SD	0.8	1.0	244	1.3	2.2	606	1.1	1.4	776	2.1	1.4	1269	1.8	1.4	735
15	Mean	15.5	18.3	2341	18.4	21.0	3718	21.1	23.3	5462	22.1	24.2	6230	24.6	25.8	8214
	SD	1.5	1.6	650	2.1	1.6	816	1.9	2.2	1204	1.7	2.2	1464	1.6	1.6	1521

*W = width (mm)

†L = length (mm)

‡V = volume (mm^3)

£SD = standard deviation

Total of 57 ablations, range of 2 to 6 repeat measurements for each setting